Hypertension

JOURNAL OF THE AMERICAN HEART ASSOCIATION

American Heart Association®

Learn and Live℠

Noninvasive Evaluation of Left Ventricular Afterload: Part 2: Arterial Pressure-Flow and Pressure-Volume Relations in Humans

Julio A. Chirinos and Patrick Segers

Hypertension 2010;56;563-570; originally published online Aug 23, 2010;
DOI: 10.1161/HYPERTENSIONAHA.110.157339
Hypertension is published by the American Heart Association. 7272 Greenville Avenue, Dallas, TX 72514

 Print ISSN: 0194-911X. Online ISSN: 1524-4563

Noninvasive Evaluation of Left Ventricular Afterload
Part 2: Arterial Pressure-Flow and Pressure-Volume Relations in Humans

Julio A. Chirinos, Patrick Segers

Abstract—The mechanical load imposed by the systemic circulation to the left ventricle is an important determinant of normal and abnormal cardiovascular function. Left ventricular afterload is determined by complex time-varying phenomena, which affect pressure and flow patterns generated by the pumping ventricle. Left ventricular afterload is best described in terms of pressure-flow relations, allowing for quantification of various components of load using simplified biomechanical models of the circulation, with great potential for mechanistic understanding of the role of central hemodynamics in cardiovascular disease and the effects of therapeutic interventions. In the second part of this tutorial, we review analytic methods used to characterize left ventricular afterload, including analyses of central arterial pressure-flow relations and windkessel modeling (pressure-volume relations). Conceptual descriptions of various models and methods are emphasized over mathematical ones. Our review is aimed at helping researchers and clinicians obtain and interpret results from analyses of left ventricular afterload in clinical and epidemiological settings. **(*Hypertension*. 2010;56:563-570.)**

Key Words: afterload ■ noninvasive ■ input impedance ■ arterial load

The mechanical load imposed by the systemic circulation to the left ventricle (LV) is an important determinant of normal and abnormal cardiovascular function. With the availability of noninvasive methods to accurately measure central pressure and flow, as well as computational tools for their analysis, there is great potential for their application in order to gain further mechanistic understanding of the role of central hemodynamics in cardiovascular disease. In the first part of this tutorial, we reviewed noninvasive methods to measure aortic pressure and flow, introduced basic concepts of analyses of pressure/flow relations in the time and frequency domains based on simple models of wave conduction and reflection, and briefly discussed wave reflections in the arterial tree. In this article, we review modeling of the arterial system as a windkessel, techniques for analyses of human arterial pressure-flow relations and considerations for interpreting hemodynamic indices in the context of research studies and individual hemodynamic assessments.

The Arterial Windkessel

In addition to considering the arterial tree as a system of tubes with wave travel and reflection (or as a transmission line network), one might address it in terms of "windkessel" model components. Frank proposed the original windkessel model as a resistance and compliance (C) pair (2-element windkessel), meant to represent small vessel resistance and large artery compliance, respectively.[1] In the arterial system, total resistance to flow originates predominantly from small arteries, whereas most of the summed compliance is provided by large arteries. This is not a perfect distinction, because large arteries impose some resistance and smaller vessels provide some compliance, whereas the model only measures total compliance ("total arterial compliance" [TAC]) and resistance ("total peripheral resistance") of the system. Compliance is the ratio between a volume change over the resulting pressure change in the system. Compliance is not equal to the ratio of stroke volume/pulse pressure, because in the arterial system, there is constant loss of volume as blood flows into the venous system. Diastole is the only time of the cycle when inflow and outflow do not occur simultaneously (inflow to the system stops with aortic valve closure) allowing volume loss to be studied in isolation. Typically, late diastole is studied to minimize the effects of wave reflections on the pressure wave. The basis of the 2-element windkessel model is that the characteristic pressure decay time during diastole is proportional to the product of resistance (R) and compliance (C). The model can be described by an exponential equation in which pressure at any given time after the initiation of diastole, $P_{dia}(t)$, is a function of pressure in end systole (or beginning of diastole, P_{es}) and the product of resistance and compliance:

$$P_{dia}(t)=P_{es}/e^{-t/RC}$$

In simple terms, this formula means that if diastolic pressure values are log transformed, pressure decay over time tends to be linearized, and the slope of this decay is proportional to the product of resistance and compliance. R can be calculated as

Received May 31, 2010; first decision June 24, 2010; revision accepted July 29, 2010.

From the Department of Medicine, Philadelphia Veterans' Affairs Medical Center-University of Pennsylvania (J.A.C.), Philadelphia, Pa; Biofluid, Tissue, and Solid Mechanics for Medical Applications (P.S.), IBiTech, Ghent University, Ghent, Belgium.

Correspondence to Julio A. Chirinos, Room 8B-111, University and Woodland Avenues, Philadelphia, PA 19104. E-mail julio.chirinos@uphs.upenn.edu

Hypertension **is available at http://hyper.ahajournals.org** **DOI: 10.1161/HYPERTENSIONAHA.110.157339**

(mean aortic pressure−mean venous pressure)/cardiac output. Venous pressure is typically neglected but should be considered in situations in which it is increased, such as heart failure. If end-systolic pressure and R are known, C can be calculated from time-resolved late diastolic pressure values. When the model is used to predict pressure waveforms based on measured flow, roughly triangular pressure waveforms are obtained, with a slow upstroke and an exponential decay in diastole. The model thus fails to explain the rapid early upstroke and the secondary peaks that occur in human pressure waveforms. It is said that the 2-element windkessel model describes the low-frequency behavior of the arterial tree (aspects related to the lower harmonics). As such, it largely accounts for the amplitude of the pressure wave, in addition to its exponential diastolic decay.[1] However, the 2-element windkessel model assumes a zero critical closing pressure (although it has been shown experimentally that the pressure at which blood flow stops is non-zero) and a constant value for C, independent of operating pressure (although C depends on pressure in a nonlinear fashion). The simple model formulations presented above can be extended to account for these issues, as discussed in detail elsewhere.[2,3]

The 2-element windkessel model can also be extended with additional components to better mimic the behavior of the arterial tree. The 3-element windkessel model is such an extended model, in which the third element is characteristic impedance (Zc). This model, originally proposed by Westerhof et al,[1] can be considered "the standard" windkessel model for the systemic circulation. Additional extended models have been suggested (an interesting model being a 4-element windkessel, taking into account inertial effects of blood acceleration and deceleration).[4] A detailed discussion on these models is beyond the scope of this article, but it should be noted that, regardless of the specific method used, windkessel modeling should rely on measured volume flow (and stroke volume) rather than assumed or estimated values. Although extended windkessel models address some of the problems mentioned above and predict more realistic pressure waveforms, it is important to remember that, as lumped 1-compartment models, they still do not account for wave transmission and reflections in arterial system. This assumption of instantaneous propagation of energy within the system ("infinite pulse wave velocity" [PWV]) remains their most important limitation, because transmission delays do occur in the arterial system.

Despite these limitations, the arterial windkessel represents a useful and intuitive approach to understanding LV afterload in mid-to-late systole and explains, to a large degree, the factors that determine the arterial pressure waveform. Nevertheless, parameters derived from windkessel models should be interpreted in the context of true arterial physiology. It should be noted that pulsatile load in early systole depends on Zc rather than the total compliance of the arterial system. However, because afterload is usually evaluated in steady state, small vessel function (systemic vascular resistance [SVR]) and TAC do affect early systolic load indirectly, because they determine, through their effect on mean and diastolic pressure, respectively, the operating point at which the aortic valve opens, initiating pulsatile flow into the proximal aorta. Because wall stiffness and diameter are dependent on operating pressure, Zc (and, therefore, early systolic pulsatile load) is affected by these operating conditions.

More recently, a "hybrid" model has been proposed in which the pressure waveform is seen as the superposition of reservoir (windkessel) pressure and additional or "excess" pressure, which is attributed to wave travel and reflection.[2] This model reconciles windkessel and wave propagation views and suggests that the largest contribution to arterial pressure is provided by the reservoir component, rather than wave travel and reflection.[2,5] This model may be seen as a time-domain representation of the 3-element windkessel model,[1] and, although appealing, it is our feeling that further understanding of the model and its intrinsic assumptions is needed before it can be widely applied in clinical and epidemiological research. What is undisputed is that forward wave transmission, wave reflections, and backward wave transmission introduce a finite delay during which the distal arterial system cannot exert any direct effects on (early) ventricular systolic load.

Pressure-Flow Analyses in the Time Domain

Principles described thus far can be applied to quantify various components of LV afterload in humans. Because wave reflections are absent in early systole, early systolic pressure and flow can be interpreted according to the simplest model presented in part 1 of this tutorial (model 1). During this period of time, the early systolic change in pressure can be divided by the early systolic change in flow to compute Zc (Figure 1 A). The time point at which flow reaches 95% of its peak value (Figure 1A) can be used to reproducibly compute this ratio.[6] Alternatively, the slope of the early systolic pressure-flow relation in pressure-flow loops (with flow on the horizontal and pressure on the vertical axis), represents proximal aortic Zc (Figure 1B).

Wave reflections typically arrive at the proximal aorta in mid-to-late systole, with superimposition of reflected and incident waves. At any given time, it can be assumed that measured pressure equals the sum of forward and backward pressure and measured flow equals the sum of forward and backward flow (backward flow having a negative sign). At their arrival, wave reflections distort the relationship between pressure and flow waveforms (by increasing pressure and decreasing flow). If the slope of the pressure-flow relationship in the absence of wave reflections (ie, Zc) is known, pressure and flow waves can be quantitatively related to each other, and differences in their waveforms can be used to "decompose" the pressure signal into its forward (Pf) and reflected (backward, Pb) components. This procedure is commonly called wave separation analysis and can be mathematically described as follows:

$$Pf = (P + Q*Zc)/2$$

$$Pb = (P - Q*Zc)/2$$

In principle, the formulas above should be applied for each individual harmonic, after which all forward pressure harmonics are added to form the total forward pressure wave and

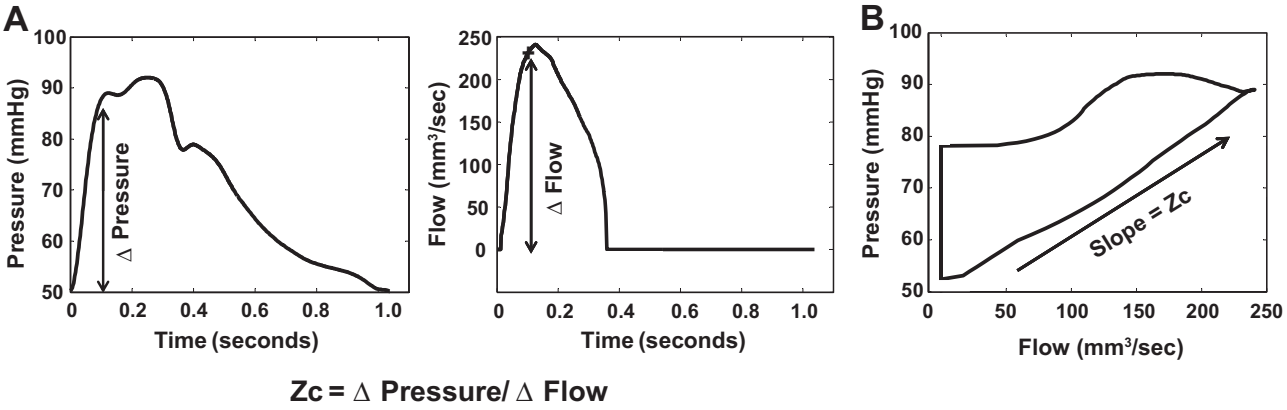

Figure 1. Computation of aortic Zc in the time domain. Because in-wave reflections are absent in early systole, early systolic pressure and flow data points can be used to measure proximal aortic Zc. We show a simple ratio of early systolic pulsatile pressure/flow when flow reaches 95% of its peak value ("+"in flow wave; A) or the slope of the early systolic pressure-flow relationship (B) equals Zc.

all backward harmonics are added to form the total backward pressure wave. In practice, however, little difference is found when simply applying these formulas to the parent pressure and flow signals.

In essence, this method is no different than "scaling" the pressure and flow waveforms to match their early systolic points (before arrival of the reflected wave) to quantify the difference in their shapes later in systole, which is attributed to wave reflections, as represented in Figure 2A (gray area). Once Pf and Pb at each time point are known, forward and reflected pressure waves can plotted (Figure 2B). The ratio of their amplitudes is the reflection magnitude:

reflection magnitude=Pb amplitude/Pf amplitude

Pressure and flow can also be used to assess TAC through various methods. Time-resolved late diastolic pressure can be used to compute C from end-systolic pressure and SVR as detailed above (2-element windkessel). We favor the pulse pressure method,[7,8] which is based on maximizing the fit between measured pulse pressure and pulse pressure predicted by the 2-element windkessel model using measured aortic flow as input. The use of the 2-element windkessel model is justified because pulse pressure is largely determined by the lower harmonics, where the 2-element windkessel model performs adequately.[1] In fact, it has been shown that the use of the 3-element windkessel model tends to overestimate TAC.[7] Another acceptable method is the area method,[3] which uses pressure-time integrals in systole and diastole to minimize the effects of high-frequency noise.[8] Finally, 3- or 4-element windkessel models can be used with measured pressure as input to estimate model parameters by maximizing the fit of predicted to measured flow or vice versa (using flow as input to maximize the fit of predicted to measured pressure). For more details regarding methods to estimate TAC, the reader is referred to an excellent review by Westerhof et al.[1]

Pressure-Flow Analyses in the Frequency Domain

For analyses in the frequency domain, pressure and flow waveforms are decomposed into their first ≈10 harmonics as discussed earlier. For each pressure-flow harmonic pair, impedance modulus is calculated as pressure modulus/flow modulus and impedance phase is computed as pressure phase minus flow phase. The resulting aortic input impedance is, therefore, a spectrum across various frequencies, with modulus and phase (Figure 3).

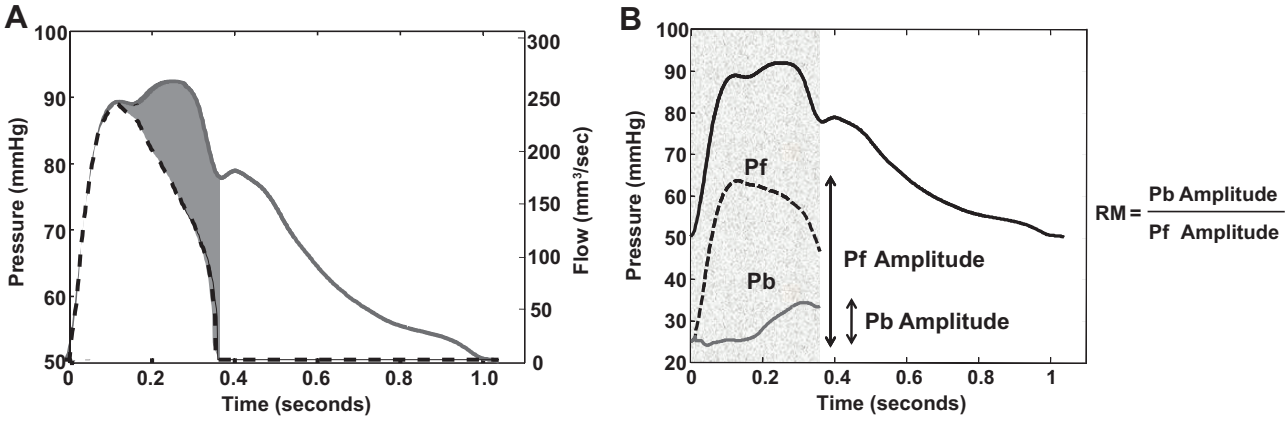

Figure 2. Wave separation analysis. Once Zc is known, pressure and flow waves can be quantitatively "scaled" in the vertical axis (A), allowing for identification of the difference in their wave forms (gray area), which is assumed to be the result of wave reflections. Pressure can be separated into forward and backward pressure (Pf and Pb), and the amplitude ratio of Pb/Pf (reflection magnitude) can be computed (B).

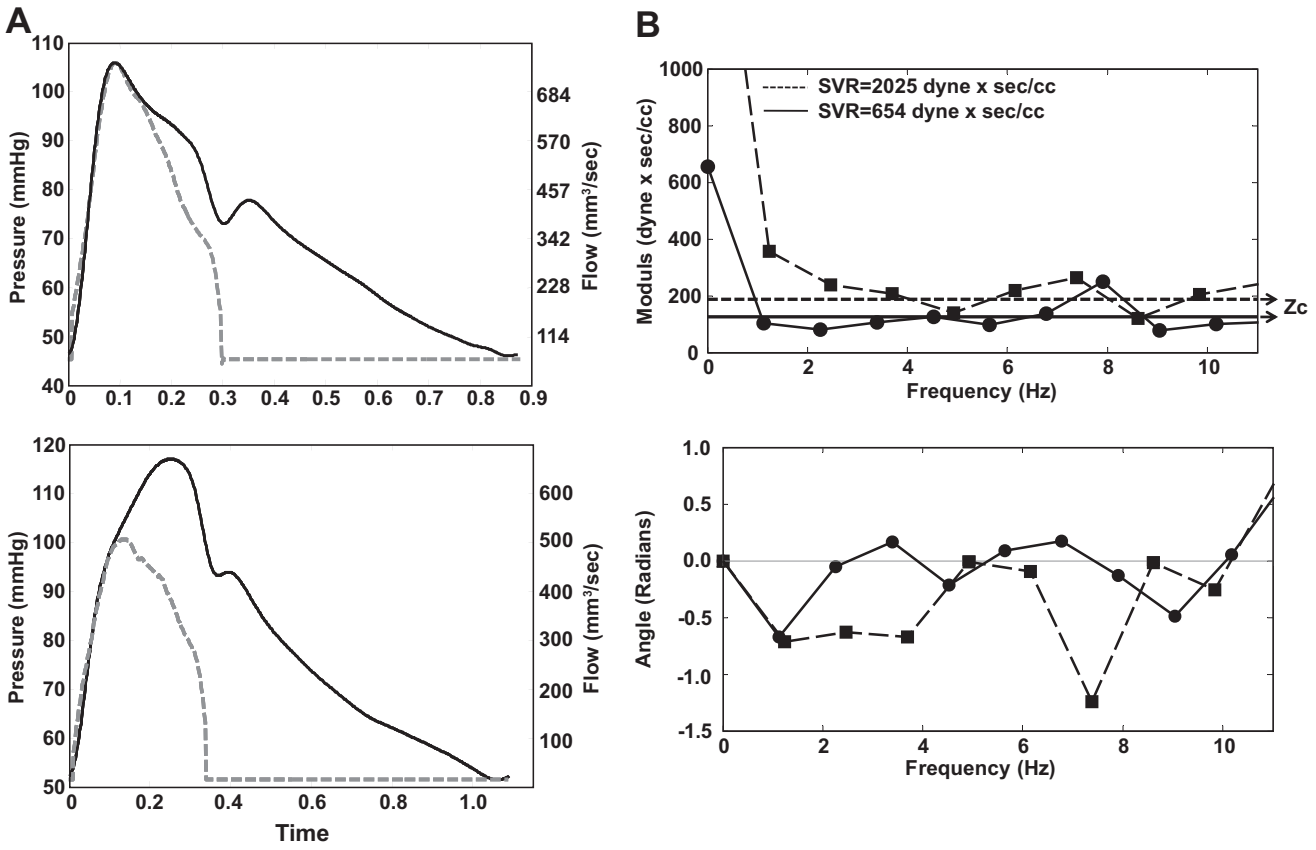

Figure 3. Examples of noninvasively obtained input impedance spectra. A, Pressure and flow measured in a normotensive 33-year–old man (top) and a hypertensive 60-year–old man (bottom). B, Modulus (top) and phase (bottom) are shown for the first 10 harmonics. SVR is the value of the 0 harmonic. The continuous and dotted lines correspond with the 33-year–old man and the hypertensive 60-year–old man, respectively. Vertical lines in the top panel represent Zc values for each individual.

The modulus of input impedance at 0 frequency is SVR. The effect of TAC is prominent at the fundamental frequency and the first few harmonics of input impedance, but disappears at high frequencies. For these lower harmonics, phase angle is negative, meaning that, at these frequencies, flow leads pressure (ie, flow peaks before pressure does), which is indicative of compliance in the system (a positive-phase angle indicates that flow lags behind pressure, indicating inertial effects). At higher frequencies, effects of inertia and compliance are balanced and combine into a resistive-like behavior, characterized by a plateau modulus value and a phase that approaches 0. The average modulus at high frequencies is aortic Zc. Random oscillations in impedance moduli about Zc are attributable to wave reflections. The first minimum of impedance modulus and first 0 crossing of phase represent the frequency at which the distance to the effective reflecting site corresponds to one quarter of the wavelength, as illustrated in part 1 of this tutorial. For example, Figure 3 shows data from a 32-year–old subject whose PWV is ≈5 m/s; first impedance minimum and 0 crossing occur at ≈2.5 Hz. Because PWV is 5 m/s, wavelength at 2.5 Hz is 2 m (5.0/2.5), indicating a "functional" reflecting site located ≈0.5 meters away from the heart. However, this is purely a functional concept rather than a true anatomic reflection site. The presence of a functionally discrete reflection site appears to be determined by complex factors related to multiple scattered terminations, including the spatial dispersion of individual reflecting sites.[9]

Considerations for the Interpretation of Afterload Indices in Clinical Research

Various indices of afterload have relatively well-defined anatomic correlates (Table and Figure 4). Most of the resistance imposed by the systemic vasculature (SVR) is thought to result from the summed resistance of small arteries and arterioles (prearteriolar vessels with diameter <500 μm).[10] Although the resistance of individual vessels is highly dependent on vessel radius (fourth power), the resistance of vascular beds depends on the arrangement of individual vessels. For vessels arranged in series, total resistance is the sum of the resistance of individual vessels. SVR can, therefore, be seen as the added resistance of large, medium, and small arteries, arterioles, capillaries, venules and veins. However, for vessels arranged in parallel, the reciprocal of their total resistance is the sum of the reciprocals of individual resistances and is always smaller than the resistance of any individual vessel. In the arterial system, vessels become progressively smaller from proximal to distal sections, which increases resistance to flow.[10] However, the number of vessels in parallel also increases, which tends to decrease overall resistance. Total resistance of individual arterial sections, therefore, partially depends on whether the number of vessels added in parallel (total

Table. Anatomic, Functional, and Structural Correlates of Arterial Load Indices

Hemodynamic Parameter	Anatomic Structure	Functional/Structural Correlate	Comments	Allometric Relationships and Indexation for Body Size[13]
Ascending aortic Zc	Proximal aorta	Inversely proportional to vessel radius$^{2.5}$ and directly proportional to square root of wall stiffness	Governs load during early ejection	Linearly and inversely related to BSA$^{0.64}$; therefore, Zc index= Zc*BSA$^{0.64}$
SVR	Arterioles (arteriolar "tone")	Resistance of individual arterioles and No. of arterioles in parallel (sensitive to arteriolar tone and rarefaction)	Nonpulsatile component of afterload; to the degree that SVR affects mean arterial pressure, it influences pulsatile load, which depends on operating pressure	Linearly and inversely related to BSA; therefore, SVR index= SVR*BSA
TAC	Large arteries and, to a lesser extent, muscular arteries and small vessels	For any given relative geometry, compliance of individual vessels is linearly proportional to vessel volume (or radius^3) and linearly and inversely proportional to wall stiffness (Young elastic modulus)	Not exclusively dependent on large arteries; does not directly affect early systolic pulsatile ventricular afterload	Linearly and directly related to BSA; therefore, TAC index=TAC/BSA
Wave reflection magnitude	Muscular arteries, resistance arterioles	Impedance mismatch between proximal and distal arterial segments; impedance mismatch depends on changes in wall stiffness and changes in total cross-sectional area (or both) between proximal and distal arterial segments	Correlate of the proportion of forward energy reflected and conducted back to the heart; effects on the LV and myocardium are dependent on its timing relative to ejection, instantaneous ventricular geometry during mid-to-late systole and LV function	Independent of body size
Wave reflection timing	Aorta (PWV) and reflection sites (muscular arteries, arterioles)	PWV is proportional to the square root of wall stiffness and the square root of vessel diameter; distance to reflection sites is linearly proportional to vessel length proximal to the reflection sites	The reflected wave appears as a discrete wave but is the resultant of many scattered reflections; a discrete functional reflection site can be identified using pressure-flow analyses, but this does not correspond with a discrete anatomic site; the reflected wave is sustained over time rather than an instantaneous phenomenon; therefore, when different landmarks of wave reflection are used to mark its onset, different results may be obtained	Linearly related to body height

cross-sectional area) can compensate for the high resistance of individual vessels with small radii. For arterioles, the effect of individual vessel radii appears to predominate over the opposing effect of total cross-sectional area, such that overall arteriolar resistance is high. In capillaries, the large total cross-sectional area is thought to predominate over the effects of individual vessel radii, resulting in a smaller overall resistance. However, it should be noted that the 3D arrangement of the microvasculature is complex, that the true location of resistance vessels in humans has not been determined with certainty, and that it may be vary in different vascular beds.[11]

As reviewed above, pulsatile load is not expressed as a single parameter but summarized using various indices derived from modeling the interaction between flow generated by the LV and the proximal aorta (Zc), arterial wave conduction and reflection (reflection magnitude and reflected wave arrival timing), and pressure-volume relations of the entire arterial tree (TAC). The Table and Figure 4 attempt to summarize anatomic and functional correlates of these indices and their effects on aortic pressure and flow, although it is useful to remember that the use of simplified mathematical models that quantify individual parameters is simply an attempt to understand complex phenomena that, in reality, are not isolated but closely interrelated. Individual parameters meant to reflect discrete functional characteristics of the arterial system may overlap with each other because of model assumptions that do not hold, true functional relationships, error measurement, or covariance because of confounding factors.

It must be recognized that different arterial indices often depend on overlapping structural and functional characteristics. For instance, although TAC is generally thought to reflect large arterial properties, medium sized and even small vessels (which are primarily responsible for the resistive component of the model) also contribute to TAC. Such overlapping characteristics should be considered when interpreting results from research studies. For example, it is possible that divergent changes in regional compliance of the aorta and smaller arteries may antagonize each other's effect on TAC. In addition, variations in stiffness, size, and relative

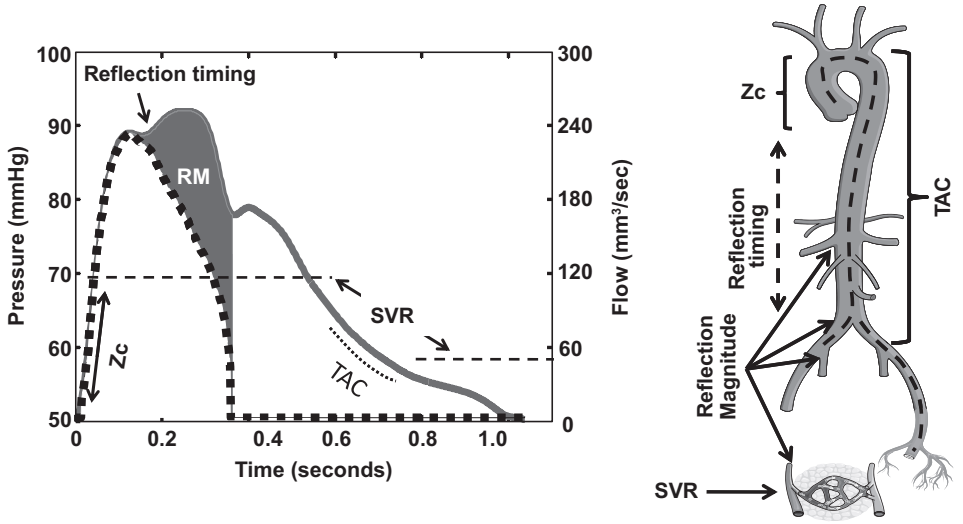

Figure 4. Anatomic correlates of various afterload indices and their effects on aortic pressure and flow in the time domain. Horizontal dashed lines indicate mean pressure and mean flow. Dashed lines in right panel are meant two represent the 2 factors affecting reflection timing (path length and pulse wave velocity).

wall geometry (vessel lumen radius versus wall thickness and vessel length versus radius) may have complex[12] effects on individual functional parameters and their statistical interplay in analyses aimed at isolating individual indices. This should be kept in mind when several indices of large artery function (eg, Zc, aortic PWV, and/or TAC) are analyzed simultaneously in regression models. In addition, statistical overlap between measured parameters may occur because their measurement errors are intrinsically related, because various indices are quantified from the same measured pressure and flow signals. This should be considered when interpreting results of multivariate linear regression, a statistical technique that does not account for correlated error. It should also be remembered that arteries become stiffer with increasing operating pressure, and, therefore, SVR may affect pulsatile load through its effects on mean (operating) pressure around which pulsatile phenomena occur. Although adjustment for mean arterial pressure is necessary when functional measurements (eg, PWV) are analyzed to assess intrinsic wall stiffness, it should be noted that the LV senses only operating load and not arterial material properties, per se.

Finally, the effect of confounders needs to be carefully eliminated. In this regard, the importance of body size cannot be overemphasized. Because cardiac output (flow) needs to increase in proportion with body size, whereas tissue perfusion pressure does not, arterial load (expressed in terms of pressure and flow) is heavily dependent on body size even in perfectly healthy adults. Adequate scaling for body size is necessary to interpret individual measurements and findings from populations. It is important to recognize that the relationship between measures of body size and arterial load may be nonlinear, making ratio-indexation or adjustment for body size in linear regression models inappropriate. One approach to solve this problem is allometric normalization using exponential powers that linearize the relationship between arterial load indices and body size measurements. With this approach, the arterial variable can be divided by the body size variable raised to an appropriate allometric exponent, therefore eliminating its normal or "expected" relationship with body size. Most indices of arterial load relate nonlinearly to body height and weight and approximately linearly to body surface area (BSA). Therefore, indexation for body surface area (Table) represents a practical approach, although the method of indexation for body size should be tailored to the specific research questions.[13] The main advantage of normalizing load for body size is that it allows for relating absolute measurements from an individual to normative data and for comparing different individuals or groups of individuals with different body size. Accounting for the normal expected relationship between body size and arterial functional variables also allows for the assessment of obesity-related abnormalities in arterial load.[13]

Resting Versus Provoked Load

Most studies have assessed LV afterload in the resting, wakeful, relaxed state, whereas daily life deviates from these experimental conditions. Therefore, laboratory provocation maneuvers may provide useful information. Aerobic exercise is normally associated with a decrease in SVR; an increase in heart rate, stroke volume, cardiac output, and mean arterial pressure; decreased reflection magnitude with earlier arrival of the reflected wave; and decreased pressure augmentation from wave reflections, without changes in Zc.[14,15] In contrast, isometric exercise is associated with an increased heart rate, unchanged or decreased stroke volume with no or little increase in cardiac output, increased SVR, increased mean arterial pressure, increased reflection magnitude with earlier wave reflections, increased Zc, and a marked decreased in TAC[16]; changes in pulsatile hemodynamics during isometric exercise are not apparent from pulse pressure measurements. Although these are average responses, great interindividual variability in these responses exists. Limited data suggest that "provoked" load may contain highly relevant information, which better correlates with hypertensive LV remodeling[16] or advanced cardiomyopathy with systolic dysfunction.[12] Assessments during the Valsalva maneuver, which minimizes

wave reflections, may also be informative. We feel that physiological provocation maneuvers should be used more widely in human arterial research. Similarly, the development of tools to assess arterial load in ambulatory settings would be highly desirable.

Interactions Among the Arteries, the Ventricle, and the Myocardium

Although indices of LV afterload are useful because they are meant to be purely reflective of arterial properties,[9] arterial load should always be interpreted by considering interactions between arteries and the LV as a pump[9,17] and also among myocardial elements, instantaneous LV geometry, and the time-varying load imposed by the arterial tree. Although indices of arterial load reflect the hydraulic load that the heart must overcome as a pump, they do not fully represent actual time-varying mechanical load (stress) experienced by contractile elements in the myocardium (myocardial afterload), which, in turn, generate the ventricular pump function. It should be noted that wall stress is the primary determinant of myocardial oxygen consumption and a key stimulus for myocardial hypertrophy and fibrosis. Wall stress not only depends on arterial properties but is profoundly affected by instantaneous LV geometry. Under normal conditions, a highly coordinated sequence of events during myocardial activation optimizes the coupling among force generation, myofiber shortening, modifications of LV geometry, endocardial excursion, cavity pressure generation, and induction of pulsatile flow toward the proximal aorta and the systemic circulation.

Although TAC is undoubtedly an important index of arterial function, distal arterial segments do not directly affect early systolic pulsatile ventricular load, because conduction delays occur in the arterial system. During this transit delay, pulsatile load is governed by the properties of the proximal aorta. It is interesting that most of the central pressure rise (pulse pressure) is achieved during this early systolic period, at a time when only ≈25% of the stroke volume has been ejected.[18] During early ejection, active development of fiber cross-bridges occurs in the electrically activated myocardium, and peak myocardial stress occurs.[19]

The hemodynamic consequences of wave reflections are highly dependent on their timing relative to the cardiac cycle. Although, on average, arrival of the reflected wave appears to occur in systole even in young adults,[20] with progressively shorter arrival times, progressively greater proportions of the reflected wave overlap with ventricular ejection, increasing LV afterload.[9] In addition, progressively smaller contributions from the reflected wave to diastolic coronary perfusion pressure occur. Although wave reflections have a predictable effect on pressure and flow as outlined in part 1 of this review, the additional afterload imposed by wave reflections may secondarily influence LV ejection during mid-to-late systole.[21] In the presence of normal LV systolic function, typical effects of the reflected wave on the aortic pressure waveform include a mid-to-late systolic shoulder, which determines an increase in peak (systolic) aortic pressure (and pulse pressure) and the area under the pressure curve during systole.[9] In the presence of LV systolic dysfunction, the load imposed by the reflected wave may be predominantly associated with a pronounced decrease and early cessation of flow[21] and shortening of the ejection period.[22]

In contrast to early systole, when systolic pressure and "diastolic" geometry (thin wall and large cavity) occur, myocardial fiber shortening and ejection of blood determine a progressive change in LV geometry, which causes a decrease in myocardial stress (despite rising pressure) during mid-to-late systole, such that wall stress tends to reach its lowest ejection-phase value in end systole.[19] This sequence of events appears to be ideal for the myocardium to handle the additional load imposed by wave reflections and may be compromised in ventricles with depressed ejection fraction. Increased mid-to-late systolic load may be particularly deleterious to the myocardium when contractility is impaired, because force-velocity relationships demonstrate that load and contractility have independent effects on myocardial shortening. Therefore, it is possible that impaired myocardial-arterial coupling occurs in the presence of even mild degrees of systolic dysfunction, and wave reflections may play a role in the progression of systolic myocardial dysfunction, which should be addressed in future studies. Future research should also address how various components of arterial load relate to time-varying myocardial stress in various disease states.

It should be noted that reflected waves may have important influences on the myocardium even in the presence of preserved LV pump function and ejection fraction. Although absolute myocardial stress is normally lower in late systole, the myocardium may be particularly vulnerable to late systolic load (as opposed to early systolic load), which may be because of intrinsic differences in cellular processes between early and late ejection. This may explain the closer association between late systolic load and ventricular hypertrophy[16] and abnormal diastolic relaxation[23] demonstrated experimentally and supported by human studies. More studies are needed to assess the roles of early and late systolic ventricular and myocardial afterload on diastolic relaxation, myocardial oxygen supply/demand, and myocardial remodeling and fibrosis. These studies may improve our understanding of hypertensive heart disease, heart failure with preserved ejection fraction and with decreased ejection fraction, valvular heart disease, and the syndrome of coronary ischemia with normal coronary angiograms. For a more extensive discussion of the consequences of afterload for the failing and nonfailing heart, the reader is referred to previous publications.[9,21]

Perspectives

The vast amount of hemodynamic knowledge accumulated over the last several decades can (and should) now be directly applied in clinical research using state-of-the-art noninvasive techniques. More observational and interventional studies are needed to characterize specific abnormalities in LV afterload and their role in disease, the effect of available therapeutic interventions on central hemodynamics, and the role of specific abnormalities as predictors of response to therapy. More studies assessing the transduction of biomechanical signals into biological phenomena (eg, myocardial hypertrophy, fibrosis, and dysfunction at the cellular level) are also needed. Population studies should continue to assess normal

and abnormal aging and its role on cardiovascular risk. Novel genomic and proteomic approaches may yield valuable insights in this regard, if combined with careful phenotyping. It should be recognized that abnormalities in arterial hemodynamic function likely play a mechanistic role in cardiovascular disease independent of atherosclerosis[24] and, therefore, may constitute a parallel, direct mechanism of risk and an opportunity for therapeutic interventions.

Despite available methods derived from careful hemodynamic research, it is clear that neither of the commonly used conceptual models fully explain central hemodynamics in all individuals. Current methods to assess wave reflections may be too simplistic and may have the potential to overestimate the importance of wave reflections as determinants of LV afterload. On the other hand, lumped models totally neglect wave reflections, which is an aberration of a physical reality. There continues to be a need to reconcile various paradigms. Recent work by Parker and colleagues[2,5] constitutes a step in this direction, although more complex modeling and a sound mathematical framework might be required to properly reconcile "slow" phenomena related to the aortic buffer and "fast" phenomena related to the superimposed propagation and reflection of longitudinal waves. Given the complexity of arterial hemodynamics, an optimal compromise between precision and simplicity should be found to provide meaningful and unequivocal information that yet can be readily implemented in clinical research and personalized approaches to the evaluation and treatment of cardiovascular disease.

Disclosures

None.

References

1. Westerhof N, Lankhaar JW, Westerhof BE. The arterial Windkessel. *Med Biol Eng Comput*. 2009;47:131–141.
2. Tyberg JV, Davies JE, Wang Z, Whitelaw WA, Flewitt JA, Shrive NG, Francis DP, Hughes AD, Parker KH, Wang JJ. Wave intensity analysis and the development of the reservoir-wave approach. *Med Biol Eng Comput*. 2009;47:221–232.
3. Liu Z, Brin KP, Yin FC. Estimation of total arterial compliance: an improved method and evaluation of current methods. *Am J Physiol*. 1986;251:H588–H600.
4. Stergiopulos N, Westerhof BE, Westerhof N. Total arterial inertance as the fourth element of the windkessel model. *Am J Physiol*. 1999;276:H81–H88.
5. Parker KH. An introduction to wave intensity analysis. *Med Biol Eng Comput*. 2009;47:175–188.
6. Mitchell GF, Tardif JC, Arnold JM, Marchiori G, O'Brien TX, Dunlap ME, Pfeffer MA. Pulsatile hemodynamics in congestive heart failure. *Hypertension*. 2001;38:1433–1439.
7. Stergiopulos N, Meister JJ, Westerhof N. Evaluation of methods for estimation of total arterial compliance. *Am J Physiol*. 1995;268:H1540–H1548.
8. Segers P, Verdonck P, Deryck Y, Brimioulle S, Naeije R, Carlier S, Stergiopulos N. Pulse pressure method and the area method for the estimation of total arterial compliance in dogs: sensitivity to wave reflection intensity. *Ann Biomed Eng*. 1999;27:480–485.
9. Nichols WW, O'Rourke MF. *McDonald's Blood Flow in Arteries. Theoretical, Experimental and Clinical Principles*. 5th ed. London, UK: Oxford University Press; Hodder Arnold; 2005.
10. Mulvany MJ, Aalkjaer C. Structure and function of small arteries. *Physiol Rev*. 1990;70:921–961.
11. Christensen KL, Mulvany MJ. Location of resistance arteries. *J Vasc Res*. 2001;38:1–12.
12. Bank AJ, Kaiser DR. Smooth muscle relaxation: effects on arterial compliance, distensibility, elastic modulus, and pulse wave velocity. *Hypertension*. 1998;32:356–359.
13. Chirinos JA, Rietzschel ER, De Buyzere ML, De Bacquer D, Gillebert TC, Gupta AK, Segers P. Arterial load and ventricular-arterial coupling: physiologic relations with body size and effect of obesity. *Hypertension*. 2009;54:558–566.
14. Murgo JP, Westerhof N, Giolma JP, Altobelli SA. Effects of exercise on aortic input impedance and pressure wave forms in normal humans. *Circ Res*. 1981;48:334–343.
15. Laskey WK, Kussmaul WG, Martin JL, Kleaveland JP, Hirshfeld JW Jr, Shroff S. Characteristics of vascular hydraulic load in patients with heart failure. *Circulation*. 1985;72:61–71.
16. Chirinos JA, Segers P, Raina A, Saif H, Swillens A, Gupta AK, Townsend R, Emmi AG Jr, Kirkpatrick JN, Keane MG, Ferrari VA, Wiegers SE, St John Sutton MG. Arterial pulsatile hemodynamic load induced by isometric exercise strongly predicts left ventricular mass in hypertension. *Am J Physiol Heart Circ Physiol*. 298:H320–H330.
17. Kawaguchi M, Hay I, Fetics B, Kass DA. Combined ventricular systolic and arterial stiffening in patients with heart failure and preserved ejection fraction: implications for systolic and diastolic reserve limitations. *Circulation*. 2003;107:714–720.
18. Mitchell GF. Clinical achievements of impedance analysis. *Med Biol Eng Comput*. 2009;47:153–163.
19. Chirinos JA, Segers P, Gupta AK, Swillens A, Rietzschel ER, De Buyzere ML, Kirkpatrick JN, Gillebert TC, Wang Y, Keane MG, Townsend R, Ferrari VA, Wiegers SE, St John Sutton M. Time-varying myocardial stress and systolic pressure-stress relationship: role in myocardial-arterial coupling in hypertension. *Circulation*. 2009;119:2798–2807.
20. Baksi AJ, Treibel TA, Davies JE, Hadjiloizou N, Foale RA, Parker KH, Francis DP, Mayet J, Hughes AD. A meta-analysis of the mechanism of blood pressure change with aging. *J Am Coll Cardiol*. 2009;54:2087–2092.
21. Westerhof N, O'Rourke MF. Haemodynamic basis for the development of left ventricular failure in systolic hypertension and for its logical therapy. *J Hypertens*. 1995;13:943–952.
22. Denardo SJ, Nandyala R, Freeman GL, Pierce GL, Nichols WW. Pulse wave analysis of the aortic pressure waveform in severe left ventricular systolic dysfunction. *Circ Heart Fail*. 2010;3:149–156.
23. Gillebert TC, Lew WY. Influence of systolic pressure profile on rate of left ventricular pressure fall. *Am J Physiol*. 1991;261:H805–H813.
24. Wilkinson IB, McEniery CM, Cockcroft JR. Arteriosclerosis and atherosclerosis: guilty by association. *Hypertension*. 2009;54:1213–1215.